Auralisation of aircraft with a synthesised emission signal based on features determined from recordings

F. Rietdijk* and K. Heutschi*

*Empa, Swiss Federal Laboratories for Materials Science and Technology, Laboratory for Acoustics/Noise Control, CH-8600 Duebendorf, Switzerland.

May 10, 2017

Abstract

Aircraft noise is a major issue in urban areas and is one of the research topics within the FP7 SONORUS project. Current methods for determining the impact of aircraft noise on annoyance and sleep disturbance are based on energetic quantities disregarding the dynamic character of the sound. To obtain a more complete representation of annoyance, listening tests with audible aircraft sound promise to determine the impact of the aircraft sound on people more accurately.

A tool was developed to auralise aircraft noise. The propagation model includes, aside from the typically considered propagation effects like Doppler shift, atmospheric attenuation and ground reflection, also amplitude and phase modulations due to atmospheric turbulence. Depending on parameters that are used to describe the atmospheric turbulence, the amplitude modulations result in clearly audible modulations and peaks in a spectrogram. Furthermore, the phase modulations cause additional decorrelation.

An inverse propagation model was developed to compute back from a receiver to source in time-domain. An automated procedure was developed to extract features from the resulting signal. These features were then used to directly synthesise the emission as function of time, and this signal was propagated to the original receiver resulting in an auralisation that should reproduce the recording it is based on.

To determine whether the auralisations indeed resembled the recordings, and thus to validate the auralisation tool, a listening test was conducted. Participants were asked to rate the similarity of two sounds in a paired comparisons. Two aircraft types were considered, and the participants were clearly able to discriminate between them, in case of both the recordings and the auralisations. However, according to the participants the auralisations did not yet fully match the recordings.

1 Introduction

1.1 Aircraft noise in urban areas

Due to the rising level of urbanization and the continuing growth of air traffic the amount of people exposed to aircraft noise increases as well. Aircraft noise can cause annoyance, sleep disturbance and stress. Annoyance is a biological process depending on multiple factors that can vary from person to person. If we consider annoyance due to sound, then certain signal components may be judged more annoying than others, but this is not reflected in energetic quantities like L_{eq} or $L_{A,max}$, although in certain cases corrections are applied. To obtain a better representation of noise we should therefore predict the audible aircraft sound and study its impact on people [8].

1.2 Auralisation

Auralisation is a method to render audible virtual sound fields [22]. The method has been used to simulate the audible sound inside rooms, but also for the sound of cars [13, 18, 19, 21, 27], trains [28], windturbines [17, 26], fans [14] and aircraft [6, 38, 39]. Auralisation of outdoor sources and environments is a key topic of the VASTCON Technical Working Group [1].

Different auralisation methods exist. Often emission synthesis and sound propagation are separated. This is not always the case because its not always possible, like e.g. when using a wave-based method [15, 16, 20].

Common methods for the emission synthesis are spectral modelling synthesis (SMS) and granular synthesis. Granular synthesis typically uses grains based on measurements and is a computationally fast method for synthesis. Spectral modelling synthesis generates a signal through a superposition of two types of signal components: tones and noise. Whereas with the granular synthesis method each grain typically corresponds directly to specific conditions, e.g. the speed of and distance to the source, with spectral modelling synthesis the synthesis strategy can be considered separate from the underlying model, and therefore a emission synthesis model can be established that relates tonal and spectral components to the operational state of the source.

1.3 Aircraft noise modelling and auralisation

Aircraft auralisation has been used to study future aircraft types [37–39] and flight procedures [40] but also to investigate the perceived unpleasantness of aircraft flyover noise as function of certain temporal parameters [25].

Aspects to consider when simulating the sound of aircraft are the different noise sources on the aircraft, the state of the aircraft and thereby the state of these sources, as well as the condition of the environment. The main noise sources of a turbojet aircraft are jet noise, fan and turbine noise, combustion noise and airframe noise. In the case of turboprop aircraft the main source is the propellor[46]. Fan or propellor noise is mostly tonal whereas the other sources are broadband noise. Which exact sources are most relevant depends on the aircraft type and flight procedure as well as the position of the source with respect to the receiver due to directivity of the sources [10].

The aircraft emission prediction tools found in the ANOPP-Source Functional Module of ANOPP2 [23, 44] and INSTANT[41], which is based on ANOPP, use established models for the noise prediction of the individual noise sources. The Heidmann model is for example used for fan noise and the Stone model for jet noise. The Heidmann model in ANOPP models five sources explicitly, of which three correspond to emission of tones and two to emission of broadband noise [6]. The model outputs for each of these five sources a spectrum in fractional-octaves. For broadband synthesis in the NAF[9], power of the tonal components in each band is divided by the amount of tones in that band. Nowadays the Heidmann model in ANOPP can output the frequencies and amplitudes of forward and aft radiated fan tones. Only Buzz-Saw noise is still output in 1/3-octaves.

Other models don't describe the contributions from the individual noise sources or spectral components but merges them together into a total spectrum. The ECAC Doc29 method [5] uses the ICAO ANP database and provides 24 1/3-octave bands, and so does CNOSSOS-EU which has adopted the 3rd edition of Doc29 [3]. The Swiss sonAIR model [48] computes an emission spectrum that is composed of two source spectra: an engine spectrum and an airframe spectrum. The current Swiss model, FLULA2, doesn't consider an emission spectrum but instead uses a database of immission spectra where propagation effects are already included [12, 42].

Aside from ANOPP2 and INSTANT none of the mentioned models make a distinction between tonal and noise contributions, thereby making them unfit for the use of aircraft auralisation which requires explicit knowledge about tonal and noise contributions.

1.4 Aircraft auralisation tool

In order to investigate annoyance and sleep disturbance due to aircraft noise a tool is needed that simulates the audible sound of aircraft in urban environments. Such a tool would require a) a model to simulate the emission of an aircraft as function of its operating conditions, b) a sound propagation model, and c) a sound reproduction setup.

For the development of the sonAIR model [48] sound recordings were made for a large amount of events nearby Zürich Airport [47]. Along with the sound recordings the position of the aircraft was registered and for a subset of the events more detailed information was obtained as well, like e.g. thrust settings. Recordings were made at multiple positions simultaneously, allowing to determine the directivity of the noise components.

To study the impact of the current flight procedures and the diverse fleet of aircraft an auralisation tool is needed that can simulate the audible sound of each of these aircraft types. Such a tool would require an emission model and it is investigated whether the sonAIR dataset can be used in conjunction with spectral modelling synthesis for a generic emission model for aircraft.

Assuming there are no modulations in the aircraft emission the synthesis strategy would require for each of the tonal components the frequency and power of the tone as well as the phase relation between the tones. For the broadband noise components the power as function of frequency would be required. These features would be needed as function of aircraft state (e.g. thrust settings, velocity) and as function of source-receiver direction in order to take into account the directivity.

In addition to a sound propagation model an automated method was developed to determine these features from the sonAIR dataset [36]. The propagation model was used to backpropagate from the source to the receiver in time-domain, undoing several of the propagation effects. From the obtained signal the previously described features were extracted.

A listening test was conducted where participants would compare recordings to auralisations that were based on the recordings and rate their similarities. For each auralisation an emission signal is generated with spectral modelling synthesis that uses as input the features that were determined with the automated method from a specific recording.

In the following sections we will discuss the different models and methods as well as the listening test setup in detail. Parameters that are given are those that were used for the stimuli in the listening test.

2 Propagation model

2.1 Overview

The propagation model takes into account geometrical spreading, Doppler shift, atmospheric attenuation and the ground reflection. Furthermore, a model was developed to include scintillations, that is, fluctuations in the sound due to atmospheric turbulence [31]. Convective amplification is supported in the propagation model but was ignored here.

Figure 1 shows a block diagram of the steps that are taken. Because of source motion all propagation effects are time-variant. The following sections will describe each of these steps in detail.

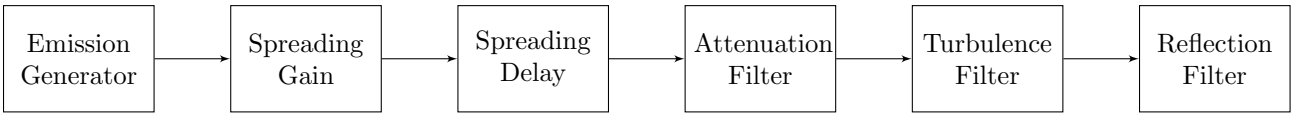

Figure 1: Block diagram of the propagation model. These steps are performed for each propagation path and the resulting signals are summed.

2.2 Geometrical spreading

Geometrical spreading causes a decrease in amplitude with distance due to divergence and increase in propagation delay with distance due to the finite speed of sound. Far field is assumed in which case we obtain the sound pressure at the receiver p_{rcv} by scaling the magnitude of the sound pressure p_{src} at some other distance from the source r_{src}

$$p_{\mathrm{rcv}} = p_{\mathrm{src}} \frac{r_{\mathrm{src}}}{r_{\mathrm{rcv}}} \tag{1}$$

The time-dependent propagation delay, which is relevant for the Doppler shift, is taken into account by resampling the discretized sound pressure signal with a Variable Delay Line. Since the signal is discrete and the delay is generally not an integer multiple of the sample time, an interpolation scheme is required.

Different interpolation schemes exist and in this case a linear interpolation scheme was chosen due to its simplicity and computational performance [17]. As a side-effect, linear interpolation causes low-pass filtering of the signal as well as aliasing. These side-effects can be minimized by choosing another interpolation scheme, like e.g. Lanczos [27, 36].

For a given sound travel time $\Delta t(t)$ from source to receiver, the index k_e of the signal $s[k_e]$ at the source time-axis is given as

$$k_e = k_r - \Delta t(t) \cdot f_s \tag{2}$$

where f_s is the sampling frequency and k_r the sample of the signal at the receiver time-axis. The received signal value s at index k_e is then determined by

$$s[k_e] = (1 - k_e + \lfloor k_e \rfloor) \cdot s\left[\lfloor k_e \rfloor\right] + (k_e - \lfloor k_e \rfloor) * s\left[\lfloor k_e \rfloor + 1\right] \tag{3}$$

where $\lfloor k_e \rfloor$ corresponds to the floor function of k_e. The sound travel time was computed with the following expression for the speed of sound $c = 343.2\sqrt{\frac{T}{T_0}}$ where T is the temperature during the event and $T_0 = 293.15$ K the reference temperature.

2.3 Atmospheric attenuation

Atmospheric attenuation is accounted for by creating a time-variant filter of length N_{aa} with a magnitude response based on ISO 9613-1:1993[2]. A single-sided magnitude spectrum is calculated as

$$H_{aa} = 10^{-d\alpha(f)/20} \tag{4}$$

where d is the source-receiver distance in meter and $\alpha(f)$ the frequency-dependent attenuation coefficient in $\mathrm{dB\,m^{-1}}$. The impulse response of a magnitude-only filter is non-causal and therefore in order to create

a causal filter a linear-phase filter corresponding to 90 degrees is added. The spectrum is real and even, and therefore the impulse response is real and even as well. After convolving the signal with the designed filter the first $N_{aa}/2$ samples were removed to account for the delay caused by the linear-phase factor.

Convolution was performed using an overlap-save algorithm. The filter length was 4096 samples and the hop size 256 samples. Transitioning to the next impulse response was done without smoothing.

2.4 Atmospheric turbulence

Fluctuations in the atmosphere of wind velocity and temperature affect sound propagation resulting in fluctuations of both the amplitude and the phase. Depending on the situation these fluctuations can be clearly audible and therefore have to be included in order to produce realistic sounding auralisations.

A method for including phase fluctuations utilizing the mutual coherence function was presented in [6, 7, 43]. The phase fluctuations cause decorrelation between the direct and ground-reflected contributions resulting in less-pronounced interference and generally more plausible auralisations.

The authors of this paper developed a model that includes both log-amplitude and phase fluctuations due to atmospheric turbulence in auralisations [31, 34, 35]. As the aircraft moves through the turbulent atmosphere, the refractive-index fluctuations are sampled by the waves propagating from source to receiver. The model considers a line-of-sight situation and assumes a frozen atmosphere. Other assumptions were a Gaussian applied turbulence spectrum and spherical wavefront [11, 45]. The model takes into account saturation of the log-amplitude fluctuations. Details about the model and how it can be used in auralisations can be found in [31].

The autocorrelation function of the Gaussian spectrum is given by [11]

$$C = \frac{\Phi\left(\rho/L\right)}{\rho/L} \tag{5}$$

and determines the shape of the log-amplitude χ and phase fluctuations S spectra. Because of the Wiener-Khinchin theorem we can take the type-1 Discrete Cosine Transform (DCT-1) to obtain the shape of the autospectra.

The autocorrelation is a function of ρ, the spatial separation between two receivers, perpendicular to the wave propagation direction, and L, the correlation length. Instead of two non-moving receivers we consider a moving source and therefore perform a space-to-time conversion to obtain $C(\tau)$ and $\rho = v_\perp \tau$ where $v_\perp$ is the speed of the aircraft perpendicular to the wave propagation direction.

Gaussian white noise is shaped with this spectrum through a convolution to obtain log-amplitude and phase fluctuations. Time-variance of the speed is taken into account not by updating the filter but instead by resampling the sequence of fluctuations using a Variable Delay Line with a delay based on the time-varying transverse speed.

At this point the fluctuations have a variance of 1. The fluctuations are scaled by the square root of the desired variances [11]

$$\sigma_\chi^2 = \sigma_S^2 = \frac{\sqrt{\pi}}{2}\sigma_\mu^2 k^2 dL \tag{6}$$

which are a function of the variance of the refractive-index fluctuations σ_μ^2, wavenumber k, source-receiver distance d and correlation length L. This scaling can be time-variant.

The fluctuations are relatively slow, and therefore a filter is constructed to apply the log-amplitude fluctuations as this also allows to take into account the frequency-dependency of the fluctuations as shown in equation 6. This filter is obtained by taking the Inverse Discrete Fourier Transform (IDFT) of $\exp(\chi)$. From equation 6 it also follows that the phase-fluctuations have a linear-phase. Therefore, the phase fluctuations are converted to a propagation delay fluctuation and applied with a Variable Delay Line.

The variance of the dynamic refractive-index σ_μ^2 was 3×10^{-5} and the correlation length L 10 m. The sequences of fluctuations were initially computed at 100 Hz. The autocorrelation filter had a length of 8192 samples. The time-variant filter for the amplitude modulations had 512 samples and hop size was 128 samples. The impulse response transitions were not smoothed.

2.5 Ground reflection

While the Image Source Method [24] was implemented with image receivers instead of image sources, we consider here only one additional path, a ground reflection, and therefore won't go into details about the implementation of the ISM.

The ground reflection is considered as a second propagation path using a mirror receiver. For the ground reflected path the same emission signal was used as for the direct path, thereby ignoring directivity of the sources. Why the directivity of the source is ignored will become clear in the following sections.

A filter was included to take into account the transfer funtion of the ground. For the ground reflection the plane wave reflection coefficient was used

$$R = \frac{Z\cos\theta - 1}{Z\cos\theta + 1} \tag{7}$$

with impedance Z calculated using Delany and Bazley's 1-parameter model

$$Z = 1 + 9.08\left(\frac{1000f}{\sigma}\right)^{-0.75} - 11.9j\left(\frac{1000f}{\sigma}\right)^{-0.73} \tag{8}$$

which is a function of frequency and flow resistivity σ. The scenarios considered were landings. Because the area around the airport consists mostly of grass a flow resistivity of $2 \times 10^5\,\mathrm{Pa\,s\,m^{-2}}$ was chosen. The filter length was 4096 samples and the hop size 256 samples.

3 Backpropagation and emission synthesis

3.1 Measurement data

For the emission synthesis a signal is generated that is based on measurements conducted as part of the sonAIR project [47]. Measurements of sound were conducted at various positions nearby Zürich Airport. An optical tracking system consisting of two camera's was used to determine the position of the aircraft in close vicinity of the aircraft.

For the data presented in this paper measurements from only a single microphone was used, situated at a height of 4 meters. Figure 2 shows an overview of the airport, the trajectory and the receiver. Aircraft were taking off and their height steadily increased from 30 to 260 meters.

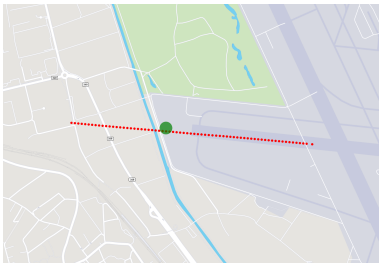

Figure 2: Overview of the airport, trajectory and the receiver. The receiver (green dot) is situated slightly north of the trajectory, almost straight underneath the trajectory.

3.2 Backpropagation

An automated procedure was developed to backpropagate from receiver to source in time-domain. The procedure assumes there is only one propagation path, the direct path, and that the aircraft can be considered a point source. As shown in Figure 3 the backpropagation algorithm undoes atmospheric attenuation, the Doppler shift, and geometrical spreading (magnitude) in that specific orderand using the methods as described in the previous section [36]. Because only the direct path was considered all parameters that were used in the backpropagation were based on values corresponding to that path.

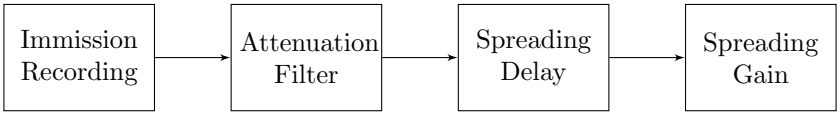

Figure 3: Block diagram of the backpropagation model. These steps are applied sequentially to a recording in order to obtain a signal in time-domain that corresponds to the emission of the aircraft.

After application of the backpropagation algorithm, a time-domain signal is obtained that corresponds to the emission of the aircraft. The influence of the ground reflection is non-negligible. A soft ground is still relatively hard and therefore a -3 dB correction was applied.

Figures 4 and 5 show spectrograms of respectively the recording and of the signal that was backpropagated. The signal after backpropagation is shorter than the recording due to lack of aircraft position information during the initial propagation delay. Aside from small variations the tonal components remain constant in frequency over time in Figure 5. The variations are caused by uncertainties in the measured position of the aircraft and thus the estimated propagation delay.

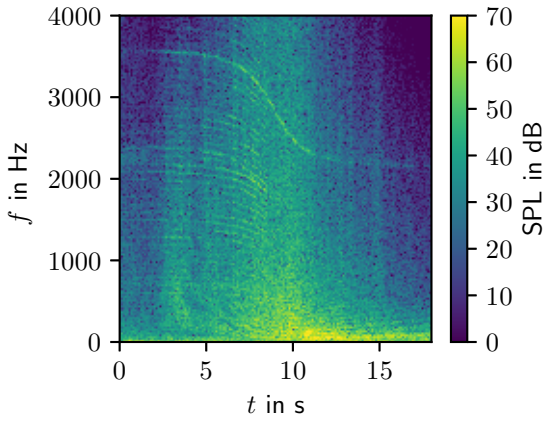

Figure 4: Spectrogram of a recording of an A320. Clearly visible are the Doppler-shifted tones and the peaks due to atmospheric turbulence. Interference between direct and reflected path acts as a Comb filter resulting in an acoustical Lloyd's mirror-effect, which can be seen here at lower frequencies. The most powerful tone corresponds to the blade passing frequency of the fan. The other tones are Buzz-Saw tones.

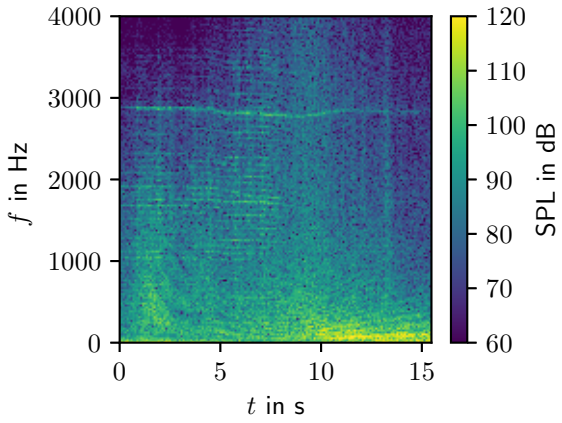

Figure 5: Spectrogram of the recording in 4 after backpropagation to the source. The Doppler-shift has mostly been removed. Artifacts like the mirror-effect and amplitude modulations due to atmospheric turbulence remain.

3.3 Feature extraction

Spectral modelling synthesis was chosen as emission synthesis strategy. With spectral modelling synthesis a signal is generated as a superposition of tones and (bandpass-filtered) noise. Therefore, a method is needed to extract from the backpropagated recordings the frequency, phase, and level of the tones, as well as the level of the noise as function of frequency.

A tone-seeking algorithm (in frequency domain) was developed [32] that utilises ISO 1996-2:2007 Annex C [4]. The tone-seeking algorithm as described in the standard did not prove capable of detecting all tones, and therefore an improved method was needed. The tones in the spectra considered, typically consist of only Buzz-Saw and blade pass frequency harmonics. Therefore, the assumption was made that

all tones found by the tone-seeking algorithm from the standard were harmonics and that the fundamental frequency was within a specified range.

The fundamental frequency is given by

$$f_0 = \gcd\left(f_1, f_2, \ldots, f_n\right) \tag{9}$$

where gcd is the *greatest common divisor*. Implementations of the gcd attempt to find an exact solution. Due to errors in the estimation of the frequency of the tones and because some tones are not harmonics, an exact solution does not exist. Given an initial estimate of the fundamental frequency, one could define an error as the sum of the squared deviation between the target order of the harmonics and the actual (inaccurate) order

$$e = \sum_{i=0}^{n} \left(\frac{f_i}{f_0} - \text{round}\left(\frac{f_i}{f_0}\right)\right)^2 \tag{10}$$

An estimate of the fundamental frequency is obtained by minimizing this error.

An earlier version of the algorithm did not use the gcd in combination with the optimisation algorithm but instead determined the fundamental frequency using the complex cepstrum [36]. While it was possible to reliably determine the fundamental frequency with the complex cepstrum, the value that was obtained was not sufficiently accurate for determining higher harmonics.

In the method as described in Annex C of ISO 1996-2:2007 each spectral line is assigned a label, e.g. whether the line is part of a tone or noise. Tones typically have a bandwidth and can therefore, depending on the frequency resolution, be spread over multiple lines. In order to compute the level of a tone, the spectral lines corresponding to that tone need to be integrated.

The bandwidth of the tonal components depends on various aspects, like frequency or phase modulations at the source or during propagation, e.g. due to atmospheric turbulence. The direct and reflected contribution are Doppler-shifted slightly differently and that causes either double peaks or a single broader peak. But also averaging time and window shape play a role.

The center frequencies of the tonal components obtained with the enhanced method were fed back in the method of the standard to obtain labels for each spectral line and to compute the levels of the tones and the noise. A value for the phase could not be obtained because the signal was too noisy. The lines that were assigned noise were integrated into $1/6$ octaves and for each fractional octave its level was kept.

For the feature extraction 2 seconds windows were used, without overlap. While a short window decreases frequency resolution and precision of the features, a short window was required in order to provide temporal resolution of the features. A 2 seconds window proved to be a good balance between temporal resolution and frequency resolution.

3.4 Emission and immission synthesis

With the extracted features, which were obtained as function of time and at several receiver positions, it is possible to develop an emission model that takes into account directivity.

An important question to ask is whether the extracted features and the spectral modelling synthesis is sufficient. Therefore, for a listening test auralisations of emission and immission were made based on recordings. For a specific event and receiver, the immission was backpropagated and features were extracted. These features were used to re-synthesise the emission.

The emission signal was propagated to the receiver, and a direct path and a single reflection were considered. The assumption was made that the emission is identical for the emission angles corresponding to direct and reflected path.

The feature extraction method provided frequencies and levels of tonal components as function of time. Variations in the frequencies as function of time could be observed, but with a two second window that would result in only few data points. We therefore ignored variations in frequency and computed an average value for the fundamental and each of the harmonics.

As mentioned in the previous section, values for the phase of the tones could not be obtained, and therefore values had to be chosen. Because the harmonics are Buzz-Saw noise, a phase corresponding to a sawtooth signal was initially assumed. Participants in a preliminary test found the simulations sound metallic compared to the recordings [33]. Therefore, eventually a random phase was chosen for each harmonic.

Figures 6 and 7 show spectrograms of respectively the emission synthesis and the auralisation at the receiver.

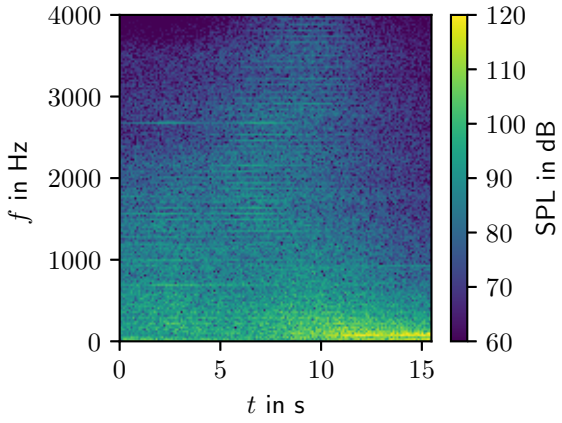

Figure 6: Emission synthesis of the aircraft. Inputs to the emission synthesiser were obtained by applying the feature-extraction algorithm to the signal shown in Figure 5. The level of the tonal components vary over time. The blade passing frequency is not clearly visible because the determined level of the tone was underestimated.

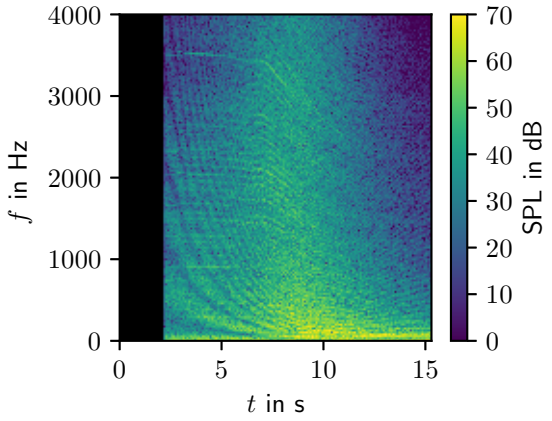

Figure 7: Auralisation of the event shown in Figure 4 . The Doppler-shifted tones and the mirror-effect are clearly visible. The Doppler-shifted tones are not very smooth. This is due to fluctuations in the aircraft position due to uncertainties.

4 Subjective validation of auralisations

4.1 Listening test

A listening test was conducted to determine whether the auralisations sound similar to the recordings they were based on. Participants were presented with pairs of stimuli and asked to rate how similar they sounded.

Eight different stimuli were considered and they were 12 seconds long. Because the sounds vary considerably over time, they were each split into parts of 4 seconds, corresponding to the approach, fly-over and distancing. For each part all combinations were considered. Each part therefore consisted of 28 pairs of stimuli of four seconds.

Of the eight stimuli four were recordings, and four were auralisations with each of them based on one of the recordings. Two aircraft types were considered, an A320 and a RJ1H, and two events per aircraft type. Headphones were used and HRTF's were not included.

Because similarity is relative, an anchor is typically used. In this test the participants were for each part first given the set of stimuli, in order to become familiar with the type of sounds and the spread in the sounds of that part, and then continued with rating the pairs. The rating was done on an eleven point Likert scale. The left side of the scale said "not so much" and the right side "very much". The scale was not numbered.

4.2 Results

The results of the participants were scaled linearly from 0 to 1 with 0 corresponding to "not so much" and 1 corresponding to "very much". Since not all participants used the full scale, they were rescaled per participant to use the full scale. There were 17 participants, all graduate students, and of which the majority studied acoustics. The results that are shown are obtained after joining the data of all participants and all three test parts.

Figure 8 shows the similarity ratings grouped per aircraft combination, considering only recordings. Figure 9 shows the similarity ratings grouped per aircraft combination, but now for the auralisations. Figures 10 and 11 show for respectively the A320 and the RJ1H the similarity ratings grouped per pairs of stimuli type, that is, recordings and/or simulations. The listening test and results can be found at respectively [29] and [30].

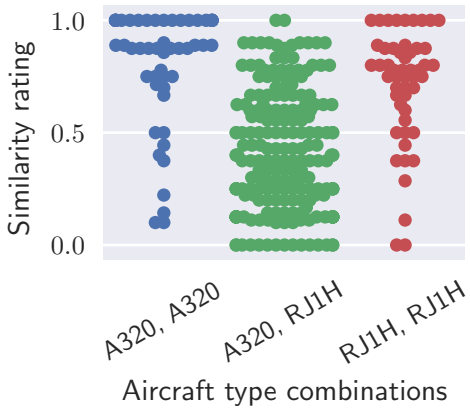

Figure 8: Similarity ratings for the recordings grouped by aircraft type.

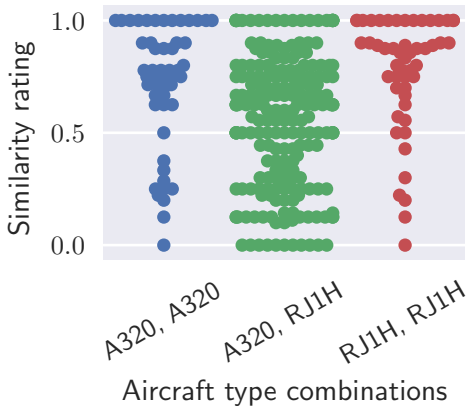

Figure 9: Similarity ratings for the auralisations grouped by aircraft type.

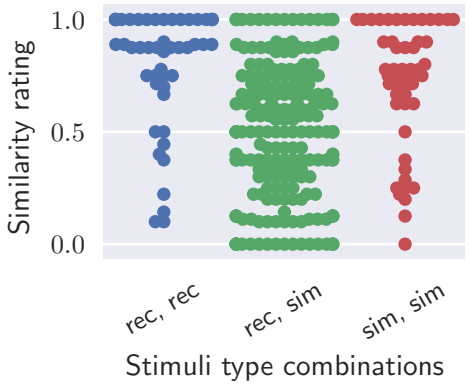

Figure 10: Similarity ratings for the A320 grouped by stimuli type combinations.

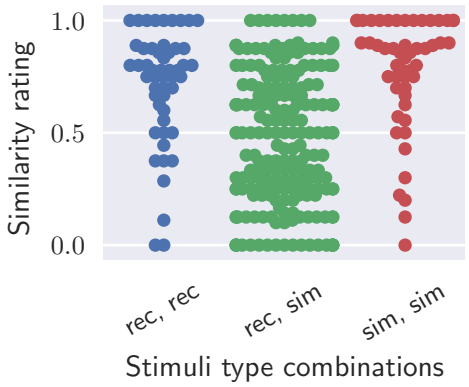

Figure 11: Similarity ratings for the RJ1H grouped by stimuli type combinations.

The ratings were obtained for three different parts of the stimuli, "start", "center" and "end", and that allows us to also group the ratings by each of these parts. Figures 12 and 13 show the similarity ratings for respectively the A320 and RJ1H grouped per stimuli type combination and per stimuli part. A Tukey boxplot is used to improve the clarity of the figure.

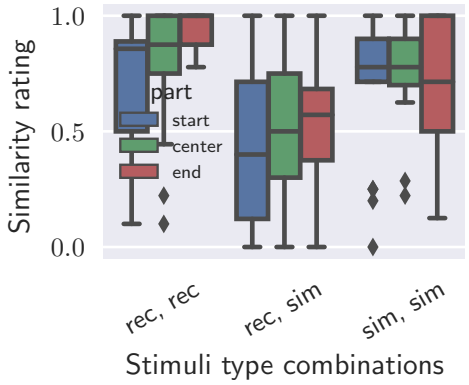

Figure 12: Similarity ratings for the A320 grouped by stimuli type combinations and stimuli part.

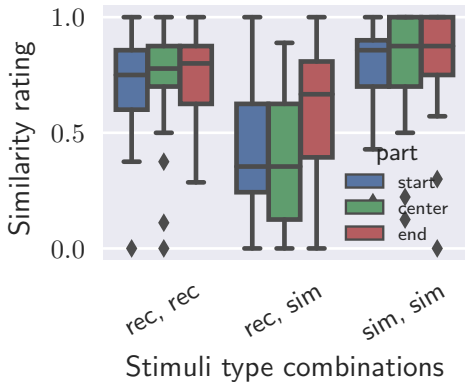

Figure 13: Similarity ratings for the RJ1H grouped by stimuli type combinations and stimuli part.

After each listening test there was a short discussion with the participant. The exact content of the discussion varied but the emphasis was on whether they noticed anything peculiar about the sounds, if they could estimate how many different aircraft they heard, and if they thought they were listening to recordings or simulations.

Participants mentioned they noted larger differences at especially the beginning of the events ("start" parts) and also at the end of the events ("end" parts). A common answer to the question how many aircraft they heard was "two or three". Occasionally, the answer would start at "two" but go to "two or more" after they were told they were listening to not only recordings but also simulations. Some participants were surprised when told that simulations were included, others said they had thought so, and a few of the participants were already aware the test was possibly going to contain simulations.

5 Discussion

As can be seen in Figure 8, the A320's are judged to be very similar to each other, and the RJ1H's as quite similar to each other. The A320's are not rated as very similar to the RJ1H's and therefore we conclude that the participants can discriminate between the two aircraft types.

In the case of the auralisations, Figure 9, the participants can also discriminate between the aircraft types, but now the RJ1H's are judged to be relatively more similar than the A320's. Compared to the recordings the difference between the A320's and the RJ1H's is slightly smaller.

Figures 10 and 11 show as additional information how similar the auralisations are to the recordings. The groups "(rec, sim)" contain pairs consisting of a recording and an auralisation. The similarity ratings for these two groups are similar to the "(A320, RJ1H)" groups in Figures 8 and 9. Therefore, it would appear that listeners can discriminate between aircraft types, but that the auralisations are considered to be of different aircraft types than the recordings they're based on.

Figures 12 and 13 show the same data but now further grouped by stimuli part. Judging from Figure 12 there appears to be a relative large dissimilarity between the "start" parts of the A320 recordings and also between the "end" parts of the A320 auralisations. The groups "(rec, rec)" and "(sim, sim)" consist however of only 17 data points each whereas the "(rec, sim)" group has 68 data points.

The participants mentioned relatively larger differences in the stimuli that correspond to the approach of the aircraft ("start" stimuli). During the approach the tonal components are clearly audible compared to other parts of the events due to the directivity. The feature-extraction algorithm was known to underestimate the power and bandwidth of the blade passing frequency and its harmonics because the algorithm was tuned for the Buzz-Saw tones. Therefore, a likely explanation is that this underestimation of power and bandwidth is causing audible differences between recordings and auralisations.

6 Conclusion

In order to investigate the impact of aircraft sound on humans a tool was developed to auralise aircraft sound. The goal was to develop a tool that can create auralisations that sound similar to the target aircraft and is capable of creating auralisations of the current fleet of aircraft.

A propagation model based on geometrical acoustics was developed and the emission synthesis was based on features extracted from recordings with the use of an inverse propagation model and a feature extraction algorithm. A listening test was conducted to determine whether the chosen features are sufficient for creating auralisations that sound similar to the actual aircraft.

From the listening test it follows that listeners can discriminate between sounds of different aircraft types, in case of both recordings and auralisations. The similarity ratings between recordings and auralisations are similar to the similarity ratings between the two aircraft type, implying the auralisations sound like different aircraft than those that were recorded.

Therefore, future work should emphasise on further improving the simulations. The authors think that the most important point to improve is the simulation of the blade passing frequency and harmonics, and that would require a better estimation of their powers and bandwidths. Aside from that, it would seem the auralisation tool is capable of delivering plausible auralisations.

7 Acknowledgement

The research leading to these results has received funding from the People Programme (Marie Curie Actions) of the European Union's Seventh Framework Programme FP7/2007-2013 under REA grant agreement number 290110, SONORUS "Urban Sound Planner".

References

[1] VASTCON Technical Working Group. URL `https://vastcon.wordpress.com/`.

[2] ISO 9613-1:1993 - Acoustics – Attenuation of sound during propagation outdoors – Part 1: Calculation of the absorption of sound by the atmosphere. 1993. URL `http://www.iso.org/iso/iso{_}catalogue/catalogue{_}tc/catalogue{_}detail.htm?csnumber=17426`.

[3] ECAC.CEAC Doc 29, 3rd edition. Technical report, 2005.

[4] ISO 1996-2:2007 - Acoustics – Description, measurement and assessment of environmental noise – Part 2: Determination of environmental noise levels. Technical report, 2007. URL `http://www.iso.org/iso/catalogue{_}detail.htm?csnumber=41860`.

[5] ECAC.CEAC Doc 29, 4th edition. Technical report, 2016.

[6] M. Arntzen. *Aircraft noise calculation and synthesis in a non-standard atmosphere*. TU Delft, Delft University of Technology, 2014. ISBN urn:isbn:9789462594647. doi: 10.4233/uuid:c56e213c-82db-423d-a5bd-503554653413. URL `http://repository.tudelft.nl/view/ir/uuid:c56e213c-82db-423d-a5bd-503554653413/`.

[7] M. Arntzen and D. G. Simons. Ground reflection with turbulence induced coherence loss in flyover auralization. *International Journal of Aeroacoustics*, 13(5-6):449–462, 2014. ISSN 1475472X. doi: 10.1260/1475-472X.13.5-6.449. URL `http://www.scopus.com/inward/record.url?eid=2-s2.0-84913619129{&}partnerID=40{&}md5=7e7abbfff2b761722a31ac68b9b96fe1`.

[8] M. Arntzen and T. van Veen. Aircraft Noise Simulation for a Virtual Reality Environment. *17th AIAA/CEAS Aeroacoustics Conference*, 2011. URL `http://arc.aiaa.org/doi/pdf/10.2514/6.2011-2853`.

[9] A. R. Aumann, B. C. Tuttle, W. L. Chapin, and S. A. Rizzi. The NASA Auralization Framework and plugin architecture. *INTER-NOISE 2015 - 44th International Congress and Exposition on Noise Control Engineering*, page ADC 40; Institute of Noise Control Engineering of, 2015.

[10] L. Bertsch, D. G. Simons, and M. Snellen. Aircraft Noise: The major sources, modelling capabilities, and reduction possibilities. 2015. URL http://elib.dlr.de/95939/.

[11] G. A. Daigle, J. E. Piercy, and T. F. W. Embleton. Line-of-sight propagation through atmospheric turbulence near the ground. *Journal of the Acoustical Society of America*, 74(5): 1505–1513, 1983. ISSN 00014966. URL http://www.scopus.com/inward/record.url?eid=2-s2.0-0020850406{&}partnerID=tZOtx3y1.

[12] Empa. FLULA2 Ein Verfahren zur Berechnung und Darstellung der Fluglrmbelästung. 2010. URL http://www.empa.ch/plugin/template/empa/*/37718.

[13] J. Forssén, T. Kaczmarek, J. Alvarsson, P. Lundén, and M. E. Nilsson. Auralization of traffic noise within the LISTEN project Preliminary results for passenger car pass-by. In *Euronoise*, 2009.

[14] I. García Merino and K. Larsson. Auralization of outdoor fan noise in shielded areas. pages 2939–2949, 2016. URL http://ri.diva-portal.org/smash/record.jsf?pid=diva2{%}3A1059676{&}dswid=-1026.

[15] F. Georgiou and M. Hornikx. Incorporating directivity in the Fourier pseudospectral time-domain method using spherical harmonics. *The Journal of the Acoustical Society of America*, 140(2):855–865, aug 2016. ISSN 0001-4966. doi: 10.1121/1.4960467. URL http://asa.scitation.org/doi/10.1121/1.4960467.

[16] F. Georgiou and M. Hornikx. Auralisation of car pass-by using simulated impulse responses. In *Urban SOUND Planning-International Symposium*, Munich, 2016.

[17] K. Heutschi, R. Pieren, M. Müller, M. Manyoky, U. W. Hayek, and K. Eggenschwiler. Auralization of Wind Turbine Noise: Propagation Filtering and Vegetation Noise Synthesis. *Acta Acustica united with Acustica*, 100(1):13–24, 2014. ISSN 16101928. doi: 10.3813/AAA.918682. URL http://openurl.ingenta.com/content/xref?genre=article{&}issn=1610-1928{&}volume=100{&}issue=1{&}spage=13.

[18] A. Hoffmann. *Auralization, perception and detection of tyre-road noise*. PhD thesis, Chalmers University of Technology, 2016.

[19] A. Hoffmann, P. Bergman, and W. Kropp. Perception of tyre noise: Can tyre noise be differentiated and characterized by the perception of a listener outside the car? *Acta Acustica united with Acustica*, 102(6):992–998, 2016. ISSN 16101928. doi: 10.3813/AAA.919014.

[20] M. Hornikx. Ten questions concerning computational urban acoustics. *Building and Environment*, 106:409–421, sep 2016. ISSN 03601323. doi: 10.1016/j.buildenv.2016.06.028. URL http://linkinghub.elsevier.com/retrieve/pii/S0360132316302359.

[21] J. Jagla, J. Maillard, and N. Martin. Sample-based engine noise synthesis using an enhanced pitch-synchronous overlap-and-add method. *The Journal of the Acoustical Society of America*, 132(5): 3098–3108, nov 2012. ISSN 0001-4966. doi: 10.1121/1.4754663. URL http://asa.scitation.org/doi/10.1121/1.4754663.

[22] M. Kleiner, B.-I. Dalenbäck, and P. Svensson. Auralization - An Overview. *Journal of the Audio Engineering Society*, 41(11):861–875, 1993.

[23] L. V. Lopes and C. L. Burley. ANOPP2 User's Manual Version 1.2. 2016.

[24] F. Mechel. *Room Acoustical Fields*. Springer, 2013. ISBN 9783642223556.

[25] A. Paté, C. Lavandier, A. Minard, and I. Le Griffon. Perceived Unpleasantness of Aircraft Flyover Noise: Influence of Temporal Parameters. *Acta Acustica united with Acustica*, 103(1):34–47, jan 2017. ISSN 1610-1928. doi: 10.3813/AAA.919031. URL http://www.ingentaconnect.com/content/10.3813/AAA.919031.

[26] R. Pieren, K. Heutschi, M. Müller, M. Manyoky, and K. Eggenschwiler. Auralization of Wind Turbine Noise: Emission Synthesis. *Acta Acustica united with Acustica*, 100(1):25–33, jan 2014. ISSN 16101928. doi: 10.3813/AAA.918683. URL http://openurl.ingenta.com/content/xref?genre=article{&}issn=1610-1928{&}volume=100{&}issue=1{&}spage=25.

[27] R. Pieren, T. Bütler, and K. Heutschi. Auralization of Accelerating Passenger Cars Using Spectral Modeling Synthesis. *Applied Sciences*, 6(1):5, 2015. ISSN 2076-3417. doi: 10.3390/app6010005. URL http://www.mdpi.com/2076-3417/6/1/5/htm.

[28] R. Pieren, J. M. Wunderli, A. Zemp, S. Sohr, and K. Heutschi. Auralisation of Railway Noise: A Concept for the Emission Synthesis of Rolling and Impact Noise. In *InterNoise 2016*, Hamburg, 2016.

[29] F. Rietdijk. Listening test stimuli and tests, 2017. URL https://zenodo.org/record/376263.

[30] F. Rietdijk. Listening Test Results, 2017. URL https://zenodo.org/record/376268.

[31] F. Rietdijk, J. Forssén, and K. Heutschi. Generating sequences of acoustic scintillations. *Acta Acustica united with Acustica*, 103(2), 2017.

[32] F. Rietdijk. scintillations, 2016. URL https://github.com/FRidh/scintillations/releases/tag/v0.1.0.

[33] F. Rietdijk and K. Heutschi. Auralization of aircraft noise in an urban environment. In *InterNoise 2016*, pages 2877–2881, 2016. doi: 10.5281/zenodo.12642.

[34] F. Rietdijk, K. Heutschi, and J. Forssén. Modelling sound propagation in the presence of atmospheric turbulence for the auralisation of aircraft noise. In *Forum Acusticum 2014*, Krakow, 2014.

[35] F. Rietdijk, K. Heutschi, and J. Forssén. Modelling sound propagation in the presence of atmospheric turbulence for the auralization of aircraft noise. *The Journal of the Acoustical Society of America*, 136(4):2286–2286, oct 2014. ISSN 0001-4966. doi: 10.1121/1.4900268. URL http://scitation.aip.org/content/asa/journal/jasa/136/4/10.1121/1.4900268.

[36] F. Rietdijk, K. Heutschi, and C. Zellmann. Determining an empirical emission model for the auralization of jet aircraft. In *Proceedings of EuroNoise 2015*, pages 781–784, Maastricht, The Netherlands, 2015. doi: 10.5281/zenodo.15702.

[37] S. Rizzi, A. Aumann, L. Lopes, and C. Burley. Auralization of Hybrid Wing Body Aircraft Flyover Noise from System Noise Predictions. pages 1–19, 2013. URL http://arc.aiaa.org/doi/pdf/10.2514/6.2013-542.

[38] S. Rizzi. Toward Reduced Aircraft Community Noise Impact via a Perception-Influenced Design Approach. In *InterNoise 2016*, Hamburg, 2016.

[39] S. A. Rizzi, C. L. Burley, and R. H. Thomas. Auralization of NASA N+2 Aircraft Concepts from System Noise Predictions. In *22nd AIAA/CEAS Aeroacoustics Conference*, Lyon, 2016.

[40] A. Sahai, F. Wefers, S. Pick, E. Stumpf, M. Vorländer, and T. Kuhlen. Interactive simulation of aircraft noise in aural and visual virtual environments. *Applied Acoustics*, 101:24–38, jan 2016. ISSN 0003682X. doi: 10.1016/j.apacoust.2015.08.002. URL http://www.sciencedirect.com/science/article/pii/S0003682X15002169.

[41] A. K. Sahai and E. Stumpf. Incorporating and minimizing aircraft noise annoyance during conceptual aircraft design. In *20th AIAA/CEAS aeroacoustics conference Part of AVIATION forum*, 2014.

[42] B. Schäffer, S. Plüss, and G. Thomann. Estimating the model-specific uncertainty of aircraft noise calculations. *Applied Acoustics*, 84:58–72, oct 2014. ISSN 0003682X. URL http://www.sciencedirect.com/science/article/pii/S0003682X14000280.

[43] H.-C. C. Shin, C. Hall, and D. Crichton. Auralisation of turbofan engine noise components. In *Collection of Technical Papers - 12th AIAA/CEAS Aeroacoustics Conference*, volume 5, pages 2841–2854, 2006. ISBN 1563478099. URL http://arc.aiaa.org/doi/abs/10.2514/6.2006-2620http://www.scopus.com/inward/record.url?eid=2-s2.0-33845621935{&}partnerID=tZOtx3y1.

[44] B. Tuttle, A. Aumann, S. Rizzi, J. Jones, and L. Lopes. Flyover Noise Simulation Using NASA's Coupled Aircraft System Noise Prediction and Auralization Frameworks. In *NOISE-CON*, Grand Rapids, 2017.

[45] D. K. Wilson, J. G. Brasseur, and K. E. Gilbert. Acoustic scattering and the spectrum of atmospheric turbulence. *The Journal of the Acoustical Society of America*, 105(1):30–34, 1999. ISSN 00014966. doi: 10.1121/1.424594. URL http://scitation.aip.org/content/asa/journal/jasa/105/1/10.1121/1.424594.

[46] O. Zaporozhets, V. Tokarev, and K. Attenborough. *Aircraft Noise: Assessment, prediction and Control*. Spon Press (Taylor and Francis), 2011. ISBN 9780203888827. URL http://oro.open.ac.uk/32193/.

[47] C. Zellmann, J. M. Wunderli, and B. Schäffer. SonAIR - Data acquisition for a next generation aircraft noise simulation model. In *42nd International Congress and Exposition on Noise Control Engineering 2013, INTER-NOISE 2013: Noise Control for Quality of Life*, volume 1, pages 842–850. OAL-Osterreichischer Arbeitsring fur Larmbekampfung, 2013. ISBN 9781632662675. URL http://www.scopus.com/inward/record.url?eid=2-s2.0-84904458708{&}partnerID=tZOtx3y1.

[48] C. Zellmann, J. M. Wunderli, and C. O. Paschereit. The sonAIR sound source model: spectral three-dimensional directivity patterns in dependency of the flight condition. *Proceedings of the INTER-NOISE 2016 - 45th International Congress and Exposition on Noise Control Engineering: Towards a Quieter Future*, pages 786–794, 2016.